Upper Bound Analysis of the ECAE Process by Considering Strain Hardening Materials and Three-Dimensional Rectangular Dies

R. Luri

C. J. Luis Pérez
e-mail: cluis.perez@unavarra.es

Manufacturing Engineering Section,
Mechanical, Energetics and Materials
Engineering Department,
Public University of Navarre,
Campus de Arrosadia s/n,
31006 Pamplona, Spain

Equal channel angular extrusion (ECAE) or pressing is a process used to introduce severe plastic deformations to processed materials with the aim of improving their mechanical properties by reducing the grain size. At present, there are no analytical studies that have considered strain hardening materials in order to determine the required force to carry out the process. All the existing papers have only considered nonstrain hardening materials. Furthermore, all those studies have been done by considering plane strain conditions. In this work, an upper bound analysis of the required force for performing the ECAE process is made by considering a full three-dimensional geometry with a rectangular cross section. From this analysis, the influence of the geometric and the material parameters is studied by considering both friction and strain hardening materials. By using the upper bound method, an analytical formulation was obtained and the influence of all the parameters was determined. With this work, it is possible to have a wider knowledge of the influence of the main affecting parameters in the ECAE process and to optimize them. [DOI: 10.1115/1.2844590]

Keywords: ECAE, upper bound, strain hardening, SPD

1 Introduction

Equal channel angular extrusion (ECAE) is a severe plastic deformation process [1] that allows us to obtain mechanical improvements due to the accumulation of plastic strain, which leads to grain size reduction [2].

The parts are extruded through two channels that intersect at angles usually between 90° and 115°, as can be observed in Figs. 1(*a*) and 1(*b*). As the material crosses the intersection between both channels, it accumulates plastic strain. In each extrusion, deformation can reach values higher than $\varepsilon > 1$ [3].

The main advantage of the ECAE process in comparison with other deformation processes is that the deformation can be imparted to the material without significant changes in the original dimensions of the workpiece. This is possible because the cross sections of both the entrance and the exit channels are manufactured with almost the same dimensions. As the dimensions of the processed billet are unchanged, it can be extruded again. This allows us to process the billet several times; hence, more accumulated strain can be achieved.

Iwahashi et al. [4] proposed the die geometry that can be seen in Fig. 2. In this configuration, the internal radius is very sharp and the external radius is not tangent to the walls of the channel.

A die design with tangent fillet radii, which improve attained deformation values, was first proposed by C. J. Luis [5], and the analytical strain expression was determined. Another ECAE die configuration was proposed by Luri et al. [6], and it was demonstrated that the fillet radius has to be tangent to allow the correct flow of the material. If a sharp internal radius is used, the material gets needlessly damaged, introducing cracks in the processed part, which is the case in the Iwahashi configuration. Moreover, it was demonstrated that by increasing the internal radius, the strain imparted to the material is higher than that obtained by using the geometry shown in Fig. 2. Therefore, as was demonstrated in Refs. [5] and [6], the processed materials reach higher deformation values with less damage by using the new ECAE geometries shown by Figs. 1(*a*) and 1(*b*) than by using the geometry from Fig. 3.

Moreover, as the fillet radii are tangent and the radii are not sharp, the stresses that the die has to support are much smaller, which leads to longer die life and less wear. On the other hand, the machining process to manufacture these dies is not very complicated; hence, it makes no sense to use a die design that has the above mentioned drawbacks. Therefore, in this work, upper bound analysis is made for the optimized ECAE dies, which are shown in Figs. 1(*a*) and 1(*b*).

When the ECAE process is carried out at high temperature, the strain hardening of the material is almost negligible. In these

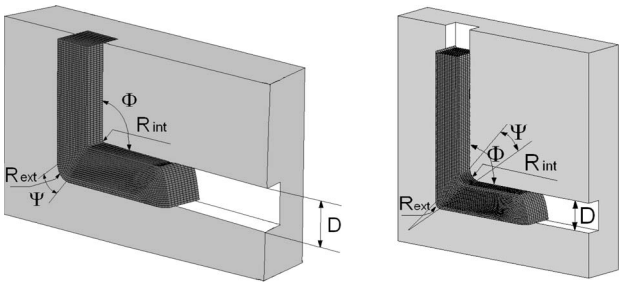

(*a*) (*b*)

Fig. 1 (*a*) **ECAE die when** $R_{int} < R_{ext}$. (*b*) **ECAE die when** $R_{int} < R_{ext}$.

Contributed by the Manufacturing Engineering Division of ASME for publication in the JOURNAL OF MANUFACTURING SCIENCE AND ENGINEERING. Manuscript received October 5, 2006; final manuscript received January 7, 2008; published online August 14, 2008. Review conducted by Jian Cao.

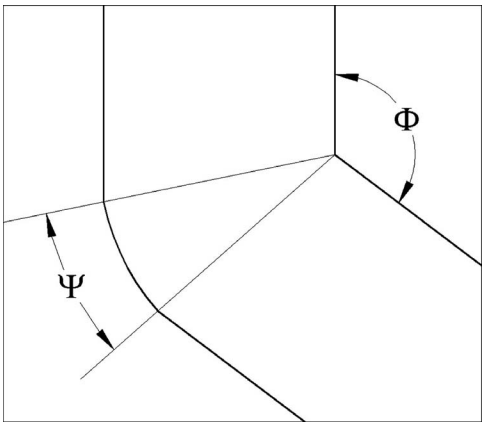

Fig. 2 Iwahashi's ECAE die geometry

cases, the process can be studied by using a material model having constant flow stress [7]. Nevertheless, when the process is carried out at room temperature, the strain hardening can have a great influence on the required force to perform the process; hence, in order to model the process, a strain hardening material has to be considered.

Up to now, all the previously published studies to obtain an expression to determine the extrusion pressure have been performed by considering plane strain assumptions. Analytical studies such as those of Refs. [1,8] do not consider strain hardening, which may lead to differences between the analytical formulas and the actual results when the material is processed at room temperature.

In this work, a three-dimensional study is carried out for the first time, taking into consideration strain hardening in order to determine the influence of the process parameters when the ECAE is performed at room temperature.

2 Determination of an Admissible Velocity Field

First of all, a kinematical admissible field has to be obtained to apply the upper bound theorem. In order to do that, a study of the velocity of the particles in the die channels has been made.

In Figs. 3(*a*) and 3(*b*), the streamline for a particle (p) is shown. The stream can be constructed by drawing two lines at both the entrance and the exit channel, which are parallel to the channel wall lines, and both of them are placed at the same distance (x) in a perpendicular direction to the channel walls. The circular part of the streamline can be obtained by drawing an arc of circumference, which is tangent to both lines.

By this streamline construction, the center of the arc (O') changes from one streamline to another, and the radius curvature (r) changes as the distance (x) changes from the internal radius when $x=0$ to the external radius when $x=D$, where D is the width of the channel at both the entrance and the exit channel.

This means that the material completely fills the channel, and as velocity changes gradually between the entrance and the exit, the discontinuities in the velocity field are avoided, as shown later.

The position of this particle can be expressed by using a Cartesian base (x,y,z) with the origin in (O), as the addition of two vectors in Eq. (1) shows. As the material is extruded, the particle (p) describes the streamline that can be seen in these figures, and as this happens, the (φ) angle increases. This means that the (φ) angle depends on time while the other parameters do not,

$$\{\overline{\mathbf{OP}}\}_{xyz} = \{\overline{\mathbf{OO'}}\}_{xyz} + \{\overline{\mathbf{O'P}}\}_{xyz} \tag{1}$$

where the vector $\{\overline{\mathbf{O'P}}\}_{xyz}$ can be expressed by Eq. (2), and the (r), (x), and (φ) parameters were as previously defined in Figs. 3(*a*) and 3(*b*),

$$\{\overline{\mathbf{O'P}}\}_{xyz} = [-r\cos\varphi; -r\sin\varphi; 0]_{xyz} \tag{2}$$

The vector $\{\overline{\mathbf{OO'}}\}_{xyz}$ can be written as

$$\{\overline{\mathbf{O'O}}\}_{xyz}\begin{cases}[-O'O_x; -O'O_y; 0]_{xyz} & \text{if } R_{\text{int}} < R_{\text{ext}} \\ [O'O_x; O'O_y; 0]_{xyz} & \text{if } R_{\text{int}} > R_{\text{ext}}\end{cases} \tag{3}$$

By substituting Eqs. (2) and (3) in Eq. (1) and by making the derivation in the Cartesian base (x,y,z) and in an inertial reference, the velocity of point (p) can be obtained from

$$\left\{\frac{d\{\overline{\mathbf{O'P}}\}}{dt}\right\}_{xyz} = \begin{cases}\begin{Bmatrix}\frac{d}{dt}(-OO'_x - r\cos\varphi)\\ \frac{d}{dt}(-OO'_y - r\sin\varphi)\\ 0\end{Bmatrix}_{xyz} & \text{if } R_{\text{int}} < R_{\text{ext}} \\ \begin{Bmatrix}\frac{d}{dt}(OO'_x - r\cos\varphi)\\ \frac{d}{dt}(OO'_y - r\sin\varphi)\\ 0\end{Bmatrix}_{xyz} & \text{if } R_{\text{int}} > R_{\text{ext}}\end{cases} = \begin{Bmatrix} r\frac{d\varphi}{dt}\sin\varphi \\ -r\frac{d\varphi}{dt}\cos\varphi \\ 0\end{Bmatrix}_{xyz} = r\frac{d\varphi}{dt}[\sin\varphi; -\cos\varphi; 0] \tag{4}$$

Equation (5) can then be obtained by expressing the velocity of particle (p), shown by Eq. (4), in cylindrical coordinates,

$$\{V(p)\}_{r\varphi z} = \left[0; r\frac{d\varphi}{dt}; 0\right] \tag{5}$$

If the velocity of the punch during the extrusion is maintained constant with a value of (V_0), the velocity at the entrance is $V(p)=V_0$ and, hence, the angular velocity can be determined from

$$V_0 = r\frac{d\varphi}{dt} \Rightarrow \frac{d\varphi}{dt} = \frac{V_0}{r} \tag{6}$$

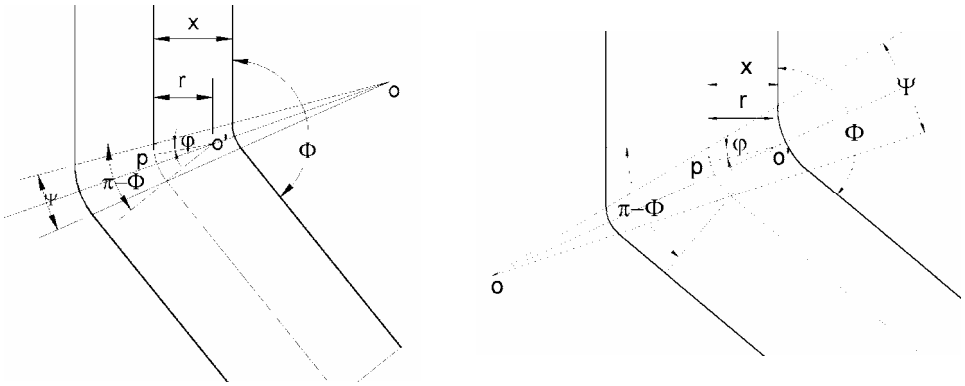

(*a*) (*b*)

Fig. 3 (*a*) **ECAE die when $R_{int} < R_{ext}$.** (*b*) **ECAE die when $R_{int} < R_{ext}$.**

$$\dot{\varepsilon}_{rr} = \frac{\partial V_r}{\partial r} = 0, \quad \dot{\varepsilon}_{\varphi\varphi} = \frac{V_r}{r} + \frac{1}{r}\frac{\partial V_\varphi}{\partial \varphi} = 0, \quad \dot{\varepsilon}_{zz} = \frac{\partial V_z}{\partial z} = 0$$

$$\dot{\varepsilon}_{r\varphi} = \frac{1}{2}\left(\frac{1}{r}\frac{\partial V_r}{\partial \varphi} + \frac{\partial V_\varphi}{dr} - \frac{V_\varphi}{r}\right) = -\frac{1}{2}\frac{V_0}{r}, \tag{7}$$

$$\dot{\varepsilon}_{\varphi x} = \frac{1}{2}\left(\frac{1}{r}\frac{\partial V_z}{\partial \varphi} + \frac{\partial V_\varphi}{\partial z}\right) = 0$$

As can be observed, the velocity of particle (p) is the same when R_{ext} is greater than R_{int} as when R_{ext} is less than R_{int}. By using the expressions that appear in Eq. (7), the strain rate tensor can then be calculated. This tensor can be expressed in principal axes as

$$\dot{\varepsilon}_{ij} = \begin{bmatrix} 0 & -\frac{1}{2}\frac{V_0}{r} & 0 \\ -\frac{1}{2}\frac{V_0}{r} & 0 & 0 \\ 0 & 0 & 0 \end{bmatrix} \Rightarrow (\text{pricipal axes}) \Rightarrow \dot{\varepsilon}_{ij} = \begin{bmatrix} \frac{1}{2}\frac{V_0}{r} & 0 & 0 \\ 0 & 0 & 0 \\ 0 & 0 & -\frac{1}{2}\frac{V_0}{r} \end{bmatrix} \tag{8}$$

As can be observed from Eq. (8), the volume incompressibility condition is satisfied. From this velocity field, it can be stated that the velocity changes gradually, from the entrance channel to the exit channel; hence, there are no velocity discontinuities, as is the case with actual velocity fields. This gradual change of velocity is due to the tangent radii of the die. If radii are not tangent to the channel, then an abrupt change of velocity will appear. This can be mathematically described as a variation of velocity in a surface discontinuity. As is widely known, when an abrupt change appears in the material flow, more damage is caused. In addition, the proposed velocity field provides a complete filling of the channel die during the extrusion. If the extrusion velocity is constant, then Eq. (9) can be used,

$$\varphi = \int_0^t \frac{d\varphi}{dt}dt = \frac{d\varphi}{dt}t + C_1 = \frac{d\varphi}{dt}t \tag{9}$$

where C_1 is a constant. In order to determine its value, an initial condition must be used. When $t=0$, the (φ) angle must be zero, that means that the constant (C_1) is equal to zero.

If t_f is the time spent by the particle to cover the intersection angle $(\pi\text{-}\Phi)$ and (t) is the time that particle (p) needs to cover the angle (φ), it can be demonstrated that the time (t) can be expressed as

$$\left.\begin{array}{l} (\pi - \Phi) = \dfrac{d\varphi}{dt}t_f \\ \varphi = \dfrac{d\varphi}{dt}t \end{array}\right\} \Rightarrow t = t_f\frac{\varphi}{(\pi - \Phi)} \tag{10}$$

The equivalent plastic strain can be expressed as

$$\bar{\varepsilon} = \int_0^t \dot{\bar{\varepsilon}}dt = \dot{\bar{\varepsilon}}t + C_2 = \dot{\bar{\varepsilon}}t \tag{11}$$

where C_2 is a constant. In order to determine its value, an initial condition must be used. When $t=0$, $(\bar{\varepsilon})$ must be zero, which means that the constant (C_2) is equal to zero.

Equation (12) can be obtained by substituting Eq. (10) in Eq. (11),

$$\bar{\varepsilon} = \dot{\bar{\varepsilon}}t_f\frac{\varphi}{(\pi - \Phi)} = C_3\frac{\varphi}{(\pi - \Phi)} \tag{12}$$

where C_3 is a constant. In order to determine its value, an initial condition must be used. When the particle (p) covers from $\varphi=0$ to $\varphi=(\pi\text{-}\Phi)$, the total equivalent plastic strain $(\bar{\varepsilon})$ is equal to $(\bar{\varepsilon}_f)$, which can be calculated by using Eqs. (13) and (14). These equations were calculated in Ref. [6],

$$\bar{\varepsilon}_f = \begin{cases} \frac{1}{\sqrt{3}} \cdot \left[2\cot\left(\frac{\Phi}{2}+\frac{\Psi}{2}\right) + (\pi-\Phi)\left[1-\cot\left(\frac{\Phi}{2}+\frac{\Psi}{2}\right)\cdot\tan\left(\frac{\Phi}{2}\right)\right]\right] & \text{if } R_{\text{int}} < R_{\text{ext}} \\ \frac{1}{\sqrt{3}} \cdot \left[2\cot\left(\frac{\Phi}{2}-\frac{\Psi}{2}\right) + (\pi-\Phi)\left[1-\cot\left(\frac{\Phi}{2}-\frac{\Psi}{2}\right)\cdot\tan\left(\frac{\Phi}{2}\right)\right]\right] & \text{if } R_{\text{int}} > R_{\text{ext}} \end{cases} \tag{13}$$

$$\Psi = \begin{cases} 2\tan^{-1}\left[\frac{(R_{\text{ext}}-R_{\text{int}})\tan\left(\frac{\Phi}{2}\right)}{D+R_{\text{int}}-R_{\text{ext}}+D\tan^2\left(\frac{\Phi}{2}\right)}\right] & \text{if } R_{\text{int}} < R_{\text{ext}} \\ 2\tan^{-1}\left[\frac{(R_{\text{int}}-R_{\text{ext}})\tan\left(\frac{\Phi}{2}\right)}{D+R_{\text{int}}-R_{\text{ext}}+D\tan^2\left(\frac{\Phi}{2}\right)}\right] & \text{if } R_{\text{int}} > R_{\text{ext}} \end{cases} \tag{14}$$

Therefore, the total equivalent plastic strain of the material when it is placed in the position of the particle (p) can be expressed as

$$\bar{\varepsilon} = \bar{\varepsilon}_f \frac{\varphi}{(\pi-\Phi)} \tag{15}$$

3 Upper Bound Method for the ECAE Process Considering Strain Hardening Materials

When a material is deformed at room temperature, its resistance to further deformation increases, this behavior is called strain hardening. One hypothesis is to consider that the degree of hardening is a function of the plastic work. For mathematical formulation, it is assumed that the final yield locus is the same, independent of the strain path a given stress state has reached (isotropic hardening). By those assumptions taking into account, the upper bound limit can be expressed as Eq. (16), as demonstrated in Ref. [11],

$$J^* = \int_V \bar{\sigma}\dot{\bar{\varepsilon}}dV + \int_{S_r} \tau|\Delta v|ds - \int_{S_t} T_i v_i ds \tag{16}$$

where J^* is the power that must be supplied to perform the process, $\bar{\sigma}$ is the flow stress of the material, $\dot{\varepsilon}_{ij}$ is the strain rate tensor, V is the volume of the deformation zone, τ is the shear stress in the friction surfaces and in the discontinuity surfaces if they exist, $|\Delta v|$ is the relative velocity in the surfaces previously mentioned, S_Γ is the area of these surfaces, T_i is the external tension on the material, v_i is the velocity of the surfaces where the external tension appears, and S_t is the area where the external tension is applied. In ECAE, there is no external tension, so the last term is equal to zero.

By using Eq. (15) and taking a Hollomon hardening rule into consideration, Eq. (17) can then be obtained,

$$\bar{\sigma} = k\bar{\varepsilon}^n = k\bar{\varepsilon}_f^n \frac{\varphi^n}{(\pi-\Phi)^n} \tag{17}$$

By using the tensor shown by Eq. (8), the equivalent strain rate can be calculated from

$$\dot{\bar{\varepsilon}} = \sqrt{\frac{2}{3}}(\dot{\varepsilon}_1^2+\dot{\varepsilon}_2^2+\dot{\varepsilon}_3^2)^{1/2} = \frac{2}{\sqrt{3}}\dot{\varepsilon}_1 = \frac{1}{\sqrt{3}}\frac{V_0}{r} \tag{18}$$

Taking into account Eqs. (17) and (18), Eq. (16) can be written as

$$FV_0 = \int_V \frac{1}{\sqrt{3}} k\bar{\varepsilon}_f^n \frac{V_0}{r}\frac{\varphi^n}{(\pi-\Phi)^n}dV + \int_{S_r} \tau|\Delta v|ds \tag{19}$$

The second term of Eq. (19) is the power lost by the flow of material when it has to go through the discontinuity surfaces and the power lost by the friction force that exists between the interface of the workpiece and the die.

As previously mentioned in the kinematical study, the velocity changes progressively from the entrance channel to the exit channel, so there are no discontinuity surfaces in this modeling, which means that the integral of the second term is extended to the interface between the part and the billet. Considering a Tresca friction model, which is given by Eq. (20), Eq. (19) can then be rewritten as Eq. (21) shows,

$$\tau = m\frac{\bar{\sigma}}{\sqrt{3}} \tag{20}$$

$$FV_0 = \int_V \frac{1}{\sqrt{3}} k\bar{\varepsilon}_f^n \frac{V_0}{r}\frac{\varphi^n}{(\pi-\Phi)^n}dV + \int_{S_r} m\frac{\bar{\sigma}}{\sqrt{3}}|\Delta v|ds \tag{21}$$

The material is deformed at the intersection between both channels, so the integral of the first term is extended to that region. The differential of volume can be deduced from Figs. 4(a) and 4(b) and is expressed mathematically in

$$dV = \begin{cases} w\frac{r}{\sin\left(\frac{\Phi}{2}+\frac{\Psi}{2}\right)}d\varphi dx & \text{if } R_{\text{int}} < R_{\text{ext}} \\ w\frac{r}{\sin\left(\frac{\Phi}{2}-\frac{\Psi}{2}\right)}d\varphi dx & \text{if } R_{\text{int}} > R_{\text{ext}} \end{cases} \tag{22}$$

where r, x, Ψ, and Φ have been previously defined in Figs. 1(a), 1(b), 3(a), 3(b), 4(a), and 4(b), and w is the dimension in the perpendicular direction to the symmetry plane.

The r radius is related to x. By observing Figs. 5(a) and 5(b), the relationship between both r and x can be obtained from

$$\begin{aligned} r &= R_{\text{int}} + x\left[1-\cot\left(\frac{\Phi}{2}+\frac{\Psi}{2}\right)\tan\left(\frac{\Phi}{2}\right)\right] \quad \text{if } R_{\text{int}} < R_{\text{ext}} \\ r &= R_{\text{int}} + x\left[1-\cot\left(\frac{\Phi}{2}-\frac{\Psi}{2}\right)\tan\left(\frac{\Phi}{2}\right)\right] \quad \text{if } R_{\text{int}} > R_{\text{ext}} \end{aligned} \tag{23}$$

The first term in Eq. (21) can be calculated from

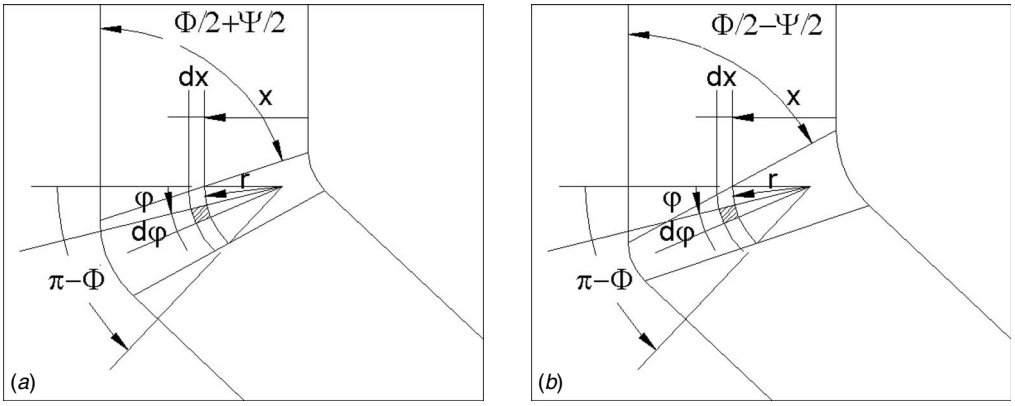

Fig. 4 (*a*) **ECAE die when** $R_{int} < R_{ext}$. (*b*) **ECAE die when** $R_{int} < R_{ext}$.

$$\int_V \frac{1}{\sqrt{3}} k\bar{\varepsilon}_f^n \frac{V_0}{r} \frac{\varphi^n}{(\pi-\Phi)^n} dV = \begin{cases} \displaystyle\int_0^D \int_0^{\pi-\Phi} \frac{1}{\sqrt{3}} k\bar{\varepsilon}_f^n \frac{V_0}{r} \frac{\varphi^n}{(\pi-\Phi)^n} w \frac{r}{\sin\left(\frac{\Phi}{2}+\frac{\Psi}{2}\right)} d\varphi dx & \text{if } R_{int} < R_{ext} \\ \displaystyle\int_0^D \int_0^{\pi-\Phi} \frac{1}{\sqrt{3}} k\bar{\varepsilon}_f^n \frac{V_0}{r} \frac{\varphi^n}{(\pi-\Phi)^n} w \frac{r}{\sin\left(\frac{\Phi}{2}-\frac{\Psi}{2}\right)} d\varphi dx & \text{if } R_{int} > R_{ext} \end{cases}$$

$$= \begin{cases} \displaystyle\frac{1}{n+1} \frac{k\bar{\varepsilon}_f^n}{\sqrt{3}} V_0 (\pi-\Phi) \frac{wD}{\sin\left(\frac{\Phi}{2}+\frac{\Psi}{2}\right)} & \text{if } R_{int} < R_{ext} \\ \displaystyle\frac{1}{n+1} \frac{k\bar{\varepsilon}_f^n}{\sqrt{3}} V_0 (\pi-\Phi) \frac{wD}{\sin\left(\frac{\Phi}{2}-\frac{\Psi}{2}\right)} & \text{if } R_{int} > R_{ext} \end{cases} \tag{24}$$

In order to calculate the second term in Eq. (21), the integral has to be separated into three integrals: one for the entrance channel, one for the intersection between both channels, and another one for the exit channel. The material in the entrance channel has an equivalent stress constant and is equal to the yield stress (σ_y) of the processed material. In the intersection between both channels, the material is progressively deformed, and hence the equivalent stress increases, following a Hollomon stress hardening rule, which has been considered as the flow stress of the processed materials. It should be pointed out that this procedure is also applicable in the case of considering different flow stress rules for the processed materials. In the exit channel, the material has to have approximately the stress of the hardening material, that is, $\bar{\sigma}_f = k\bar{\varepsilon}_f^n$, and hence the second term of Eq. (21) can be expressed as

$$\begin{aligned} \int_{S_r} m \frac{\bar{\sigma}}{\sqrt{3}} |\Delta v| ds &= m \int_{S_{entrance}} \frac{\sigma_y}{\sqrt{3}} V_0 ds_{entrance} \\ &+ m \int_{S_{entrance}} \frac{k\varepsilon_f^n}{\sqrt{3}} \frac{\varphi^n}{(\pi-\Phi)^n} V_0 ds_{intersection} \\ &+ m \int_{S_{exit}} \frac{k\varepsilon_f^n}{\sqrt{3}} V_0 ds_{exit} \end{aligned} \tag{25}$$

In order to calculate the integrals contained in Eq. (25), some parameters have to be considered. In Figs. 6(*a*) and 6(*b*), the parameters L_{ext}, $L_{R_{int}}$, $L_{R_{ext}}$, $L_{entrance}$, and L_{exit} are defined for both ECAE dies with R_{ext} higher than R_{int} and ECAE dies with R_{int} higher than R_{ext}. In both cases, w is the width in the perpendicular direction to the symmetry plane.

The parameter L_{ext} can be expressed as a function of the width of the channel (D) and the fillet radii (R_{ext}) and (R_{int}) as Eq. (21) shows,

$$\begin{aligned} L_{ext} &= D \cot\left(\frac{\Phi}{2}+\frac{\Psi}{2}\right) \quad \text{if } R_{int} < R_{ext} \\ L_{ext} &= D \cot\left(\frac{\Phi}{2}-\frac{\Psi}{2}\right) \quad \text{if } R_{int} > R_{ext} \end{aligned} \tag{26}$$

By solving Eq. (25) for ECAE dies having $R_{int} < R_{ext}$, Eq. (27) is obtained, as shown in the Appendix,

$$\begin{aligned} &= m \frac{\sigma_y}{\sqrt{3}} V_0 \left(2wL_{entrance} + wD \cot\left(\frac{\Phi}{2}+\frac{\Psi}{2}\right) + 2DL_{entrance} \right. \\ &\left. + D^2 \cot\left(\frac{\Phi}{2}+\frac{\Psi}{2}\right) \right) + m \frac{k\varepsilon_f^n}{\sqrt{3}} V_0 \left(2wL_{exit} + wD \cot\left(\frac{\Phi}{2}+\frac{\Psi}{2}\right) \right. \\ &\left. + 2DL_{exit} + D^2 \cot\left(\frac{\Phi}{2}+\frac{\Psi}{2}\right) \right) + m \frac{1}{\sqrt{3}} \frac{k\varepsilon_f^n}{n+1} V_0 w (R_{int} + R_{ext})(\pi \\ &- \Phi) + m \frac{2}{\sqrt{3}} \frac{k\varepsilon_f^n}{n+1} (\pi-\Phi) V_0 \left(\frac{R_{int}+R_{ext}}{2} \right) \frac{D}{\sin\left(\frac{\Phi}{2}+\frac{\Psi}{2}\right)} \end{aligned} \tag{27}$$

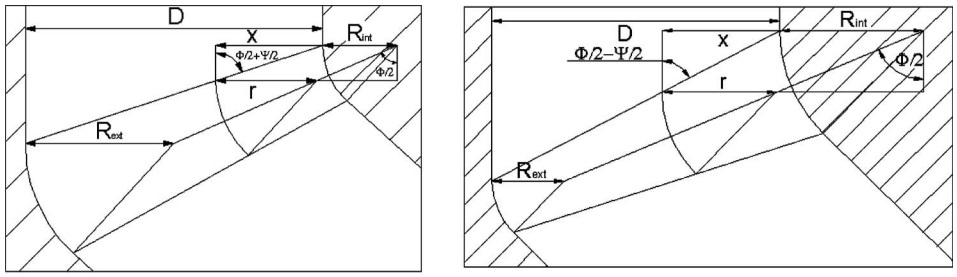

Fig. 5 (*a*) **Geometric parameters for determining the relationship between** r **and** x **in the ECAE dies with** $R_{int} < R_{ext}$. (*b*) **Geometric parameters for determining the relationship between** r **and** x **in the ECAE dies with** $R_{int} > R_{ext}$.

By following the same procedure as before, the second term of Eq. (21), considering ECAE dies having $R_{int} > R_{ext}$, can be calculated from

$$
\begin{aligned}
&= m\frac{\sigma_v}{\sqrt{3}}V_0\left(2wL_{\text{entrance}} + wD\cot\left(\frac{\Phi}{2} - \frac{\Psi}{2}\right) + 2DL_{\text{entrance}}\right.\\
&\left. + D^2\cot\left(\frac{\Phi}{2} - \frac{\Psi}{2}\right)\right) + m\frac{k\varepsilon_f^n}{\sqrt{3}}V_0\left(2wL_{\text{exit}} + wD\cot\left(\frac{\Phi}{2} - \frac{\Psi}{2}\right)\right.\\
&\left. + 2DL_{\text{exit}} + D^2\cot\left(\frac{\Phi}{2} - \frac{\Psi}{2}\right)\right)\\
&+ m\frac{1}{\sqrt{3}}\frac{k\varepsilon_f^n}{n+1}V_0 w(R_{\text{int}} + R_{\text{ext}})(\pi - \Phi)\\
&+ m\frac{2}{\sqrt{3}}\frac{k\varepsilon_f^n}{n+1}(\pi - \Phi)V_0\left(\frac{R_{\text{int}} + R_{\text{ext}}}{2}\right)\frac{D}{\sin\left(\frac{\Phi}{2} - \frac{\Psi}{2}\right)}
\end{aligned}
\tag{28}
$$

By using Eqs. (24), (27), and (28) in Eq. (21), the required force can be calculated for the ECAE process when strain hardening materials are processed. This required force is shown by

$$
\begin{aligned}
F = {} & \frac{1}{\sqrt{3}}\sigma_{\text{mean}}\frac{(\pi - \Phi)Dw}{\sin\left(\frac{\Phi}{2} + \frac{\Psi}{2}\right)} + \frac{m}{\sqrt{3}}\left(\sigma_y\left(2wL_{\text{entrance}} + wD\cot\left(\frac{\Phi}{2} + \frac{\Psi}{2}\right) + 2DL_{\text{entrance}} + D^2\cot\left(\frac{\Phi}{2} + \frac{\Psi}{2}\right)\right)\right.\\
& \left. + \sigma_f\left(2wL_{\text{exit}} + wD\cot\left(\frac{\Phi}{2} + \frac{\Psi}{2}\right) + 2DL_{\text{exit}} + D^2\cot\left(\frac{\Phi}{2} + \frac{\Psi}{2}\right)\right) + \sigma_{\text{mean}}(R_{\text{int}} + R_{\text{ext}})(\pi - \Phi)\left(w + \frac{D}{\sin\left(\frac{\Phi}{2} + \frac{\Psi}{2}\right)}\right)\right) \quad \text{if } R_{\text{int}} < R_{\text{ext}}\\
F = {} & \frac{1}{\sqrt{3}}\sigma_{\text{mean}}\frac{(\pi - \Phi)Dw}{\sin\left(\frac{\Phi}{2} - \frac{\Psi}{2}\right)} + \frac{m}{\sqrt{3}}\left(\sigma_y\left(2wL_{\text{entrance}} + wD\cot\left(\frac{\Phi}{2} - \frac{\Psi}{2}\right) + 2DL_{\text{entrance}} + D^2\cot\left(\frac{\Phi}{2} - \frac{\Psi}{2}\right)\right)\right.\\
& \left. + \sigma_f\left(2wL_{\text{exit}} + wD\cot\left(\frac{\Phi}{2} - \frac{\Psi}{2}\right) + 2DL_{\text{exit}} + D^2\cot\left(\frac{\Phi}{2} - \frac{\Psi}{2}\right)\right) + \sigma_{\text{mean}}(R_{\text{int}} + R_{\text{ext}})(\pi - \Phi)\left(w + \frac{D}{\sin\left(\frac{\Phi}{2} - \frac{\Psi}{2}\right)}\right)\right) \quad \text{if } R_{\text{int}} > R_{\text{ext}}
\end{aligned}
\tag{29}
$$

where σ_y is the yield stress of the material, σ_{mean} is the mean stress for a Hollomon material that has been deformed and which has reached an ε_f value of deformation, as shown by

$$\sigma_{\text{mean}} = \frac{1}{\varepsilon_f}\int_0^{\varepsilon_f} k\varepsilon^n d\varepsilon = \frac{1}{n+1}k\varepsilon_f^n \tag{30}$$

and σ_f is the yield stress of a Hollomon material that has accumulated a total deformation value of ε_f as can be observed in

$$\sigma_f = k\varepsilon_f'' \tag{31}$$

In extrusion processes, it is more usual to use the extrusion pressure instead of the extrusion force. So, from Eq. (29), Eq. (32) can be obtained,

$$
\begin{aligned}
\sigma = {} & \frac{1}{\sqrt{3}}\sigma_{\text{mean}}\frac{(\pi - \Phi)}{\sin\left(\frac{\Phi}{2} + \frac{\Psi}{2}\right)} + \frac{m}{\sqrt{3}}\left(\sigma_y\left(2\frac{L_{\text{entrance}}}{D} + \cot\left(\frac{\Phi}{2} + \frac{\Psi}{2}\right) + 2\frac{L_{\text{entrance}}}{D}\frac{D}{w} + \frac{D}{w}\cot\left(\frac{\Phi}{2} + \frac{\Psi}{2}\right)\right)\right.\\
& \left. + \sigma_f\left(2\frac{L_{\text{exit}}}{D} + \cot\left(\frac{\Phi}{2} + \frac{\Psi}{2}\right) + 2\frac{L_{\text{exit}}}{D}\frac{D}{w} + \frac{D}{w}\cot\left(\frac{\Phi}{2} + \frac{\Psi}{2}\right)\right) + \sigma_{\text{mean}}\left(\frac{R_{\text{int}}}{D} + \frac{R_{\text{ext}}}{D}\right)(\pi - \Phi)\left(1 + \frac{D}{w}\frac{1}{\sin\left(\frac{\Phi}{2} + \frac{\Psi}{2}\right)}\right)\right) \quad \text{if } R_{\text{int}} < R_{\text{ext}}
\end{aligned}
$$

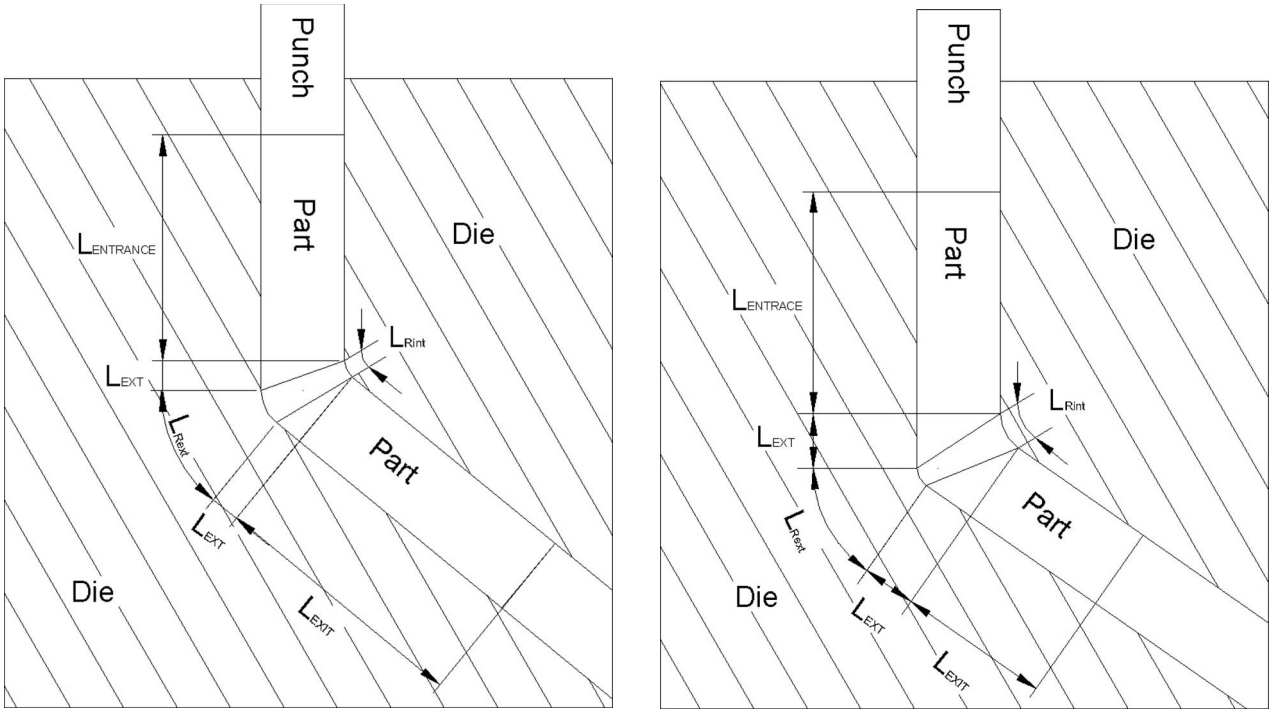

Fig. 6 (*a*) **Geometric parameters for determining the contact area in ECAE dies with $R_{int} < R_{ext}$.** (*b*) **Geometric parameters for determining the contact area in ECAE dies with $R_{int} > R_{ext}$.**

$$\sigma = \frac{1}{\sqrt{3}}\sigma_{\text{mean}}\frac{(\pi-\Phi)Dw}{\sin\left(\frac{\Phi}{2}-\frac{\Psi}{2}\right)} + \frac{m}{\sqrt{3}}\Bigg(\sigma_y\left(2\frac{L_{\text{entrance}}}{D} + \cot\left(\frac{\Phi}{2}-\frac{\Psi}{2}\right) + 2\frac{L_{\text{entrance}}}{D}\frac{D}{w} + \frac{D}{w}\cot\left(\frac{\Phi}{2}-\frac{\Psi}{2}\right)\right)$$
$$+ \sigma_f\left(2\frac{L_{\text{exit}}}{D} + \cot\left(\frac{\Phi}{2}-\frac{\Psi}{2}\right) + 2\frac{L_{\text{exit}}}{D}\frac{D}{w} + \frac{D}{w}\cot\left(\frac{\Phi}{2}-\frac{\Psi}{2}\right)\right) + \sigma_{\text{mean}}\left(\frac{R_{\text{int}}}{D}+\frac{R_{\text{ext}}}{D}\right)(\pi-\Phi)\left(1+\frac{D}{w}\frac{1}{\sin\left(\frac{\Phi}{2}-\frac{\Psi}{2}\right)}\right)\Bigg) \quad \text{if } R_{\text{int}} > R_{\text{ext}} \tag{32}$$

It is clear that L_{entrance} and L_{exit} are related because as the material disappears from the entrance channel, it appears at the exit channel. By considering the volume incompressibility of the material, Eqs. (33) and (34) can be obtained. These equations give a relationship for L_{entrance} and L_{exit} in both ECAE dies with $R_{\text{int}} < R_{\text{ext}}$ and $R_{\text{int}} < R_{\text{ext}}$,

$$L_{\text{exit}} = L_{\text{init}} - D\cot\left(\frac{\Phi}{2}+\frac{\Psi}{2}\right) - \frac{(\pi-\Phi)}{\sin\left(\frac{\Phi}{2}+\frac{\Psi}{2}\right)}\left(\frac{(R_{\text{int}}+R_{\text{ext}})}{2}\right) - L_{\text{entrance}} \quad \text{if } R_{\text{int}} < R_{\text{ext}} \tag{33}$$

$$DwL_{\text{init}} = DwL_{\text{entrance}} + DwL_{\text{exit}} + DwL_{\text{exit}} + \int_0^D\int_0^{\pi-\Phi} w\frac{r}{\sin\left(\frac{\Phi}{2}+\frac{\Psi}{2}\right)}d\varphi dx$$

$$DwL_{\text{init}} = DwL_{\text{entrance}} + DwL_{\text{exit}} + DwL_{\text{ext}} + \int_0^D\int_0^{\pi-\Phi} w\frac{r}{\sin\left(\frac{\Phi}{2}-\frac{\Psi}{2}\right)}d\varphi dx$$

$$L_{\text{init}} = L_{\text{entrance}} + L_{\text{exit}} + D\cot\left(\frac{\Phi}{2}+\frac{\Psi}{2}\right) + \frac{(\pi-\Phi)}{\sin\left(\frac{\Phi}{2}+\frac{\Psi}{2}\right)}\left(\frac{(R_{\text{int}}+R_{\text{ext}})}{2}\right)$$

$$L_{\text{init}} = L_{\text{entrance}} + L_{\text{exit}} + D\cot\left(\frac{\Phi}{2}-\frac{\Psi}{2}\right) + \frac{(\pi-\Phi)}{\sin\left(\frac{\Phi}{2}-\frac{\Psi}{2}\right)}\left(\frac{(R_{\text{int}}+R_{\text{ext}})}{2}\right)$$

$$L_{\text{exit}} = L_{\text{init}} - D\cot\left(\frac{\Phi}{2} - \frac{\Psi}{2}\right) - \frac{(\pi - \Phi)}{\sin\left(\frac{\Phi}{2} - \frac{\Psi}{2}\right)}\left(\frac{(R_{\text{int}} + R_{\text{ext}})}{2}\right) - L_{\text{entrance}} \quad \text{if } R_{\text{int}} > R_{\text{ext}} \tag{34}$$

where L_{init} is the length of the billet before the extrusion process. By using Eqs. (33) and (34) in Eq. (32), the extrusion pressure can be calculated as a function of the initial length of the part (L_{init}), the fillet radii ($R_{\text{int}}, R_{\text{ext}}$), the cross section dimensions (D, w), and the instant of the extrusion process, which is defined by the length of the material at the entrance channel (L_{entrance}), as Eq. (35) shows,

$$\sigma = \frac{1}{\sqrt{3}}\sigma_{\text{mean}}\frac{(\pi - \Phi)}{\sin\left(\frac{\Phi}{2} + \frac{\Psi}{2}\right)} + \frac{m}{\sqrt{3}}\left(\sigma_y\left(1 + \frac{D}{w}\right)\left(2\frac{L_{\text{entrance}}}{D} + \cot\left(\frac{\Phi}{2} + \frac{\Psi}{2}\right)\right)\right.$$
$$+ \sigma_f\left(\left(1 + \frac{D}{w}\right)\left(2\frac{L_{\text{init}}}{D} - \cot\left(\frac{\Phi}{2} + \frac{\Psi}{2}\right) - \frac{(\pi - \Phi)}{\sin\left(\frac{\Phi}{2} + \frac{\Psi}{2}\right)}\left(\frac{R_{\text{int}}}{D} + \frac{R_{\text{ext}}}{D}\right) - 2\frac{L_{\text{entrance}}}{D}\right)\right)$$
$$\left. + \sigma_{\text{mean}}(\pi - \Phi)\left(\frac{R_{\text{int}}}{D} + \frac{R_{\text{ext}}}{D}\right)\left(1 + \frac{D}{w}\frac{1}{\sin\left(\frac{\Phi}{2} + \frac{\Psi}{2}\right)}\right)\right) \quad \text{if } R_{\text{int}} < R_{\text{ext}}$$

$$\sigma = \frac{1}{\sqrt{3}}\sigma_{\text{mean}}\frac{(\pi - \Phi)}{\sin\left(\frac{\Phi}{2} - \frac{\Psi}{2}\right)} + \frac{m}{\sqrt{3}}\left(\sigma_y\left(1 + \frac{D}{w}\right)\left(2\frac{L_{\text{entrance}}}{D} + \cot\left(\frac{\Phi}{2} - \frac{\Psi}{2}\right)\right)\right.$$
$$+ \sigma_f\left(\left(1 + \frac{D}{w}\right)\left(2\frac{L_{\text{init}}}{D} - \cot\left(\frac{\Phi}{2} - \frac{\Psi}{2}\right) - \frac{(\pi - \Phi)}{\sin\left(\frac{\Phi}{2} - \frac{\Psi}{2}\right)}\left(\frac{R_{\text{int}}}{D} + \frac{R_{\text{ext}}}{D}\right) - 2\frac{L_{\text{entrance}}}{D}\right)\right)$$
$$\left. + \sigma_{\text{mean}}(\pi - \Phi)\left(\frac{R_{\text{int}}}{D} + \frac{R_{\text{ext}}}{D}\right)\left(1 + \frac{D}{w}\frac{1}{\sin\left(\frac{\Phi}{2} - \frac{\Psi}{2}\right)}\right)\right) \quad \text{if } R_{\text{int}} > R_{\text{ext}} \tag{35}$$

4 Discussion of Results

By using Eqs. (14) and (35), the extrusion pressure can be calculated. In Fig. 7, the force stroke of the ECAE process for an ECAE die geometry, which has $R_{\text{int}}=0.5$ mm, $R_{\text{ext}}=1.5$ mm, $D=10$ mm, $\Phi=90$ deg, $w=10$ mm, and a length of the part (L_{init}) of 80 mm, can be observed.

As can be observed, as the extrusion process is carried out, the extrusion pressure increases because of the increase of the friction force. As was previously mentioned, the contact pressure at the exit channel is higher than that at the entrance channel as a consequence of the strain hardening behavior.

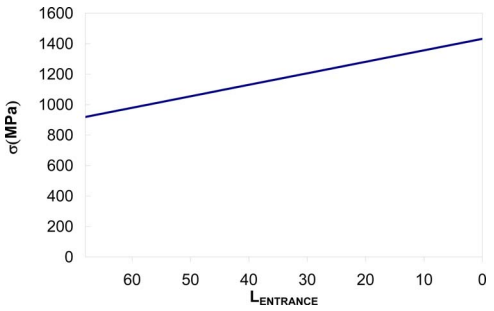

Fig. 7 Stroke curve for an CEAE die having $R_{\text{int}}=0.5$ mm, $R_{\text{ext}}=1.5$ mm, $D=10$ mm, $\Phi=90$ deg, $w=10$ mm, $L_{\text{init}}=80$ mm, $k=428.18$, $n=0.1161$, and $m=0.125$

As the material passes from the entrance channel to the exit channel, the contact pressure in the contact area between both the die and the workpiece increases, and the higher the contact pressure is, the higher the friction force, and the higher the friction force, the higher the force required to perform the process.

As can be observed in Eq. (35), the extrusion pressure depends on the material properties ($\sigma_y, \sigma_{\text{mean}}, \sigma_f$), the die geometric properties (R_{int}/D), (R_{ext}/D), (D/w), and (Φ), the part dimensions (L_{init}/D), and the shear friction coefficient (m).

From Eq. (35), it can be shown that the higher the yield stress of the processed materials and the higher the k and n values of the Hollomon material model, the higher the extrusion pressure. In this work, a 5083 aluminium alloy has been considered to obtain the different response surfaces. The material flow stress for this 5083 aluminium alloy was determined in Ref. [12] and is shown by.

$$\bar{\sigma} = 428.18\bar{\varepsilon}^{0.1161} \tag{36}$$

The friction coefficient (m) is a parameter that is difficult to control. This means that it is impossible to fix it at a desired value. From Eq. (35), it can be stated that the higher the friction coefficient, the higher the required extrusion pressure. From Eq. (13), it is possible to see that an increase in the friction coefficient does not increase the attained deformation. Therefore, the friction coefficient must be reduced as much as possible by using appropriated lubricants at the interface between the die and the part, with the aim of reducing the process force, which may cause the punch to undergo buckling.

In Ref. [12], a shear friction coefficient of approximately 0.125

Table 1 Selected intervals for the variables in the ECAE dies

$80\ \text{deg} \leqslant \Phi \leqslant 100\ \text{deg}$
$6 \leqslant \frac{L_{\text{init}}}{D} \leqslant 10$
$0 \leqslant \frac{R_{\text{int}}}{D} \leqslant 0.5$
$0 \leqslant \frac{R_{\text{ext}}}{D} \leqslant 0.5$

was obtained for an ECAE process by using MoS_2 in spray as lubricant and a 5083 aluminium alloy as the processed material.

In most of the ECAE die designs, when a rectangular cross section is considered, the relationship between D and w is the unity, which means a square cross section. Hence, for all the response surfaces shown in this work, the variable D/w is taken to be equal to 1. Furthermore, it should be pointed out that Eq. (35) allows us to estimate the required force when rectangular cross sections are used, if needed.

In order to know the influence of the geometric parameters, the intervals of variation shown by Table 1 have been considered. Typical values for ECAE dies are $D=10$ mm, $\Phi=90$ deg and the part length $L_{\text{init}}=80$ mm. These intervals have been chosen so that the most commonly used values are located in the middle of the interval.

The response surfaces are plotted in order to show how the extrusion pressure changes when two variables change, while the others are fixed at the average value of the interval.

As the extrusion pressure increases during the process, the extrusion pressure in the middle of the stroke will be used in order to compare the extrusion pressure when different ECAE die geometries are used.

As Fig. 8 shows, the higher the external radius (R_{ext}/D), the lower the extrusion pressure. As demonstrated in Ref. [6], by using Eq. (13), the higher the external radius, the lower the imparted deformation $(\bar{\varepsilon}_f)$. As the first term of Eq. (35) is related to the power employed in deforming the material, this term decreases due to the decrease of the deformation.

Also, σ_{mean} and σ_f decrease due to the decrease of the imparted deformation. This decrease reduces the second term of Eq. (35). Therefore, when the imparted deformation is reduced, both terms of Eq. (35) are decreased, and so is the extrusion force.

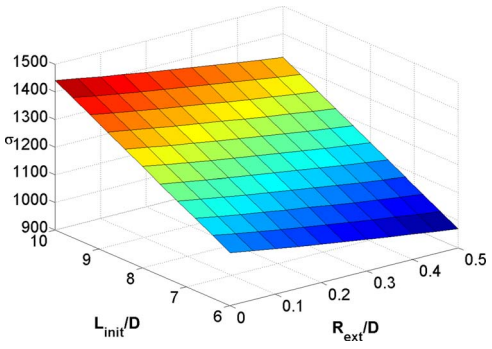

Fig. 8 Response surface of the extrusion pressure (σ) when L_{init}/D and R_{ext}/D vary and $R_{\text{int}}/D=0.25$, $\Phi=90$ deg, and $w/D=1$

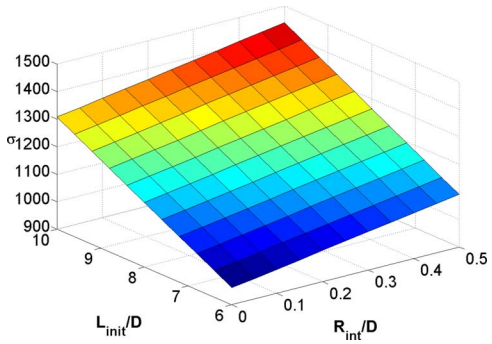

Fig. 9 Response surface of the extrusion pressure (σ) when L_{init}/D and R_{int}/D vary with $R_{\text{ext}}/D=0.25$, $\Phi=90$ deg, and $w/D=1$

In Fig. 8, it can be observed that as the length of the billet (L_{init}/D) increases, the extrusion pressure increases. The second term of Eq. (35) is related to the power wasted in overcoming the friction force. The higher the part length (L_{init}/D), the higher the interface surface between both the workpiece and the die, and hence the higher the friction force. Therefore, as the length of the part increases, the second term of Eq. (35) increases because of the increase in the friction force and hence the necessary pressure to develop the process increases.

It can be stated that there is no interaction between (R_{ext}/D) and (L_{init}/D) because of the shape of the response surface; that is to say, the variation of one of the variables does not depend on the value of the other.

As can be observed in Fig. 9, the higher the length of the part (L_{init}/D), the higher the extrusion pressure. As was previously mentioned, this is related to the increase of the interface surface and the increase in the friction force. This increase on the friction force increases the required force in the punch to carry out the process.

When the internal radius (R_{int}/D) increases, the required pressure on the punch increases. As can be deduced by using Eq. (13), the attained strain $(\bar{\varepsilon}_f)$ increases when the internal radius (R_{int}/D) increases. As was previously mentioned, when the attained strain increases, both terms of Eq. (35) increase. The first term of Eq. (35) increases because it is related to the deformation energy, and as the material reaches higher strain values, the power required increases. The second term of this equation increases because σ_{mean} and σ_f increase when the imparted deformation to the material increases. These increases entail higher extrusion pressure, as can be observed in Fig. 9. It can be affirmed from Fig. 9 that no interaction exists between variables L_{init}/D and R_{int}/D.

It can be observed in Fig. 10 that an increase in the length of

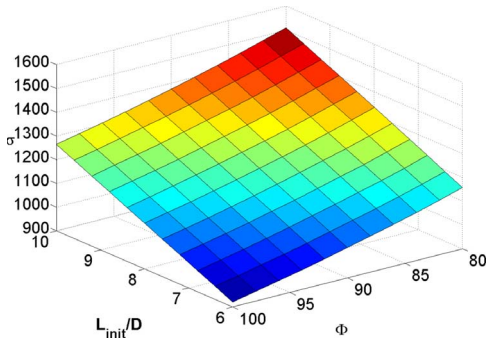

Fig. 10 Response surface of the extrusion pressure (σ) when L_{init}/D and Φ vary with $R_{\text{ext}}/D=0.25$, $R_{\text{int}}/D=0.25$, and $w/D=1$

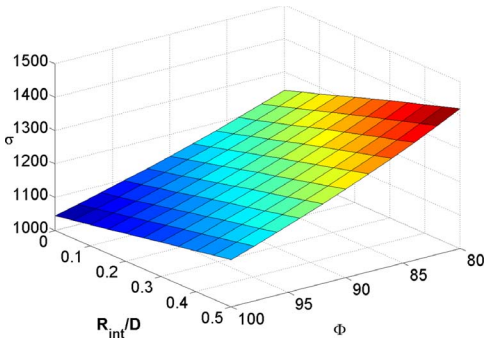

Fig. 11 Response surface of the extrusion pressure (σ) when Φ and R_{int}/D vary with R_{ext}/D=0.25, L_{init}/D=8, and w/D=1

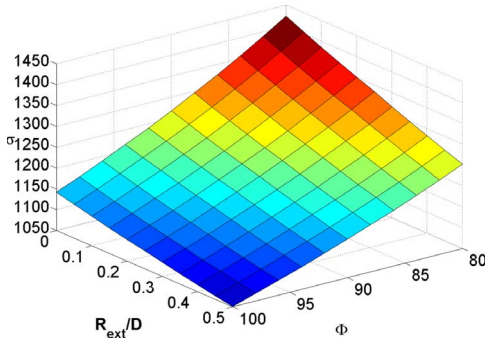

Fig. 12 Response surface of the extrusion pressure (σ) when Φ and R_{ext}/D vary with R_{int}/D=0.25, L_{init}/D=8, and w/D=1

the billet increases the required pressure to perform the process as a consequence of the increase in the friction force.

From Fig. 10 it can also be stated that the lower the intersection angle (Φ), the higher the required extrusion pressure. As can be deduced from Eq. (13), the lower the intersection angle (Φ), the higher the attained strain ($\bar{\varepsilon}_f$). This increase in the attained strain increases both terms of Eq. (35). The first term of Eq. (35) increases because it is directly linked to the deformation energy, and the second term increases because σ_{mean} and σ_f increase since they depend on the material properties and on the reached strain. The higher the reached strain the higher σ_{mean} and σ_f, and hence, a decrease on the intersection (Φ) angle makes the required force increase.

It can also be stated by observing Fig. 10, that there is no interaction between L_{init}/D and Φ.

As can be observed in Fig. 11, as the intersection (Φ) angle decreases or the internal radius (R_{int}/D) increases, the extrusion pressure increases. As was previously mentioned, as the internal radius (R_{int}/D) increases or the intersection angle (Φ) decreases, the achieved deformation ($\bar{\varepsilon}_f$) increases.

The increase in the achieved strain is a consequence of the increase of both terms of Eq. (35). The first term increases because it is linked to the energy wasted in deforming the material, and more deformation requires more power. The second term increases because of the increase of σ_{mean} and σ_f. So, as the material hardens because of the increase of strain, the contact pressure also increases, and so does the friction force; hence, the extrusion pressure has to be higher. As can be observed, due to the shape of Fig. 11, no interaction between the intersection (Φ) angle and the internal radius (R_{int}/D) is observed. This means that a variation on the intersection (Φ) angle does not change the tendency of the internal radius (R_{int}/D) and vice versa.

When both the intersection (Φ) angle or the external radius (R_{ext}/D) decrease, the extrusion pressure increases, as can be observed in Fig. 12. This behavior of the extrusion pressure can be explained from the increase of the attained strain ($\bar{\varepsilon}_f$) that the material accumulates when it is processed by using a die geometry with either a smaller intersection angle or a smaller external radius.

As can be deduced from Eq. (13), a decrease in both the intersection (Φ) angle or the external radius (R_{ext}/D) increases the reached strain ($\bar{\varepsilon}_f$), and this increases both terms of Eq. (35). As can be observed from Fig. 12, a very slight interaction between the intersection (Φ) angle and the external radius (R_{ext}/D) does exist.

When either the internal radius (R_{int}/D) increases or the external radius (R_{ext}/D) decreases, the extrusion pressure increases. This can also be explained from the increase of strain imparted to the material ($\bar{\varepsilon}_f$) when a die geometry with either higher internal radius (R_{int}/D) or lower external radius (R_{ext}/D) is used.

As can be deduced from Eq. (13), the imparted strain ($\bar{\varepsilon}_f$) increases when either the internal radius (R_{int}/D) increases or the external radius (R_{ext}/D) decreases. This increase in the attained strain ($\bar{\varepsilon}_f$) entails an increment in both terms of Eq. (35), and hence leads to an increase in the required pressure to perform the process.

As can be observed from Fig. 13, no interaction between the internal radius (R_{int}/D) and the external radius (R_{ext}/D) exists. In order to see the results more clearly and in a compact way, a summary from all of these results is presented in Table 2.

5 Conclusions

In this work, an analytical formula considering all the geometric parameters has been obtained in order to calculate the required force for performing the ECAE process. This study has been made for the first time by considering both a three-dimensional ECAE

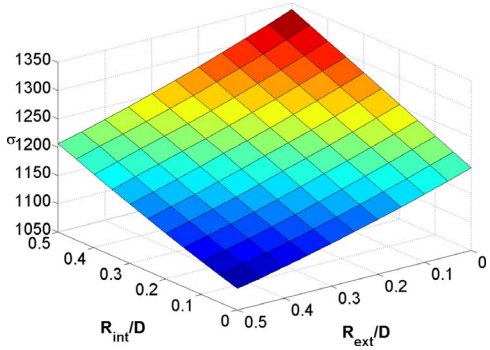

Fig. 13 Response surface of the extrusion pressure (σ) when R_{int}/D and R_{ext}/D vary with Φ=90 deg, L_{init}/D=8, and w/D=1

Table 2 Summary table

Φ	↑	σ	↓	$\bar{\varepsilon}_f$	↓
$\frac{L_{init}}{D}$	↑	σ	↑	$\bar{\varepsilon}_f$	=
$\frac{R_{int}}{D}$	↑	σ	↑	$\bar{\varepsilon}_f$	↑
$\frac{R_{ext}}{D}$	↑	σ	↓	$\bar{\varepsilon}_f$	↓
m	↑	σ	↑	$\bar{\varepsilon}_f$	=

die geometry and strain hardening materials. Therefore, with this work a precise formula for the ECAE process has been obtained.

Since the main aim of the ECAE process is to impart severe plastic deformation to the processed materials, the variables should be chosen in order to obtain higher deformation values. Nevertheless, it is also important to reduce the necessary force.

Taking these considerations into account, it can be stated that the friction coefficient should be reduced as much as possible by using appropriate lubricants since it increases the required force and does not improve the obtained strain.

Normally, when the process is going to be carried out, a volume of the material is required to be processed so D and L_{init} are fixed. It is useful to calculate the required pressure for processing the material in order to determine if the punch is going to undergo buckling or not. There are two possible limitations on the length of the billet (L_{init}): One is the pressure that the press can develop, and the other is the length of the billet which, in combination with the extrusion pressure, does not produce buckling on the punch. Nevertheless, to optimize the die shape, the main influencing design variables are (Φ), (R_{int}/D), and (R_{ext}/D). As shown in this paper, changes in these variables, which increase the reached strain, increases the required force, and hence a compromise solution should be reached.

Acknowledgment

The authors acknowledge the support given by the Ministry of Science and Technology, Spain (Research Project No. MAT2005-07732-C02-01 and Research Project No. MAT 2006-14341-C02-02).

Appendix: Development of Eq. (27)

$$
\begin{aligned}
&= m\frac{\sigma_y}{\sqrt{3}}V_0(2wL_{\text{entrance}} + wL_{\text{ext}} + 2DL_{\text{entrance}} + DL_{\text{ext}}) + m\int_0^{\pi-\Phi}\frac{k\varepsilon^n}{\sqrt{3}}V_0 wR_{\text{int}}d\varphi + m\int_0^{\pi-\Phi}\frac{k\varepsilon^n}{\sqrt{3}}V_0 wR_{\text{ext}}d\varphi \\
&+ 2m\int_0^{\pi-\Phi}\int_0^{D}\frac{k\varepsilon^n}{\sqrt{3}}V_0\frac{r}{\sin\left(\frac{\Phi}{2}+\frac{\Psi}{2}\right)}d\varphi dx + m\frac{k\varepsilon_f^n}{\sqrt{3}}V_0(2wL_{\text{exit}} + wL_{\text{ext}} + 2DL_{\text{exit}} + DL_{\text{ext}})
\end{aligned}
$$

$$
\begin{aligned}
&= m\frac{\sigma_y}{\sqrt{3}}V_0(2wL_{\text{entrance}} + wL_{\text{ext}} + 2DL_{\text{entrance}} + DL_{\text{ext}}) + m\int_0^{\pi-\Phi}\frac{k\varepsilon_f^n}{(\pi-\Phi)^n}V_0 wR_{\text{int}}d\varphi + m\int_0^{\pi-\Phi}\frac{k\varepsilon_L^n}{\sqrt{3}}\frac{\varphi^n}{(\pi-\Phi)^n}V_0 wR_{\text{ext}}d\varphi \\
&+ 2m\int_0^{\pi-\Phi}\int_0^{D}\frac{k\varepsilon_f^n}{\sqrt{3}}\frac{\varphi^n}{(\pi-\Phi)^n}V_0\frac{r}{\sin\left(\frac{\Phi}{2}+\frac{\Psi}{2}\right)}d\varphi dx + m\frac{k\varepsilon_f^n}{\sqrt{3}}V_0(2wL_{\text{exit}} + wL_{\text{ext}} + 2DL_{\text{exit}} + DL_{\text{ext}})
\end{aligned}
$$

$$
\begin{aligned}
&= m\frac{\sigma_y}{\sqrt{3}}V_0(2wL_{\text{entrance}} + wL_{\text{ext}} + 2DL_{\text{entrance}} + DL_{\text{ext}}) + m\frac{1}{\sqrt{3}}\frac{k\varepsilon_f^n}{n+1}V_0 wR_{\text{int}}(\pi-\Phi) + m\frac{1}{\sqrt{3}}\frac{k\varepsilon_f^n}{n+1}V_0 wR_{\text{ext}}(\pi-\Phi) \\
&+ 2m\int_0^{\pi-\Phi}\int_0^{D}\frac{k\varepsilon_f^n}{\sqrt{3}}\frac{\varphi^n}{(\pi-\Phi)^n}V_0\frac{R_{\text{int}} + x\left[1-\cos\left(\frac{\Phi}{2}+\frac{\Psi}{2}\right)\tan\left(\frac{\Phi}{2}\right)\right]}{\sin\left(\frac{\Phi}{2}+\frac{\Psi}{2}\right)}d\varphi dx + m\frac{k\varepsilon_f^n}{\sqrt{3}}V_0(2wL_{\text{exit}} + wL_{\text{ext}} + 2DL_{\text{exit}} + DL_{\text{ext}})
\end{aligned}
$$

$$
\begin{aligned}
&= m\frac{\sigma_y}{\sqrt{3}}V_0(2wL_{\text{entrance}} + wL_{\text{ext}} + 2DL_{\text{entrance}} + DL_{\text{ext}}) + m\frac{1}{\sqrt{3}}\frac{k\varepsilon_f^n}{n+1}V_0 wR_{\text{int}}(\pi-\Phi) + m\frac{1}{\sqrt{3}}\frac{k\varepsilon_f^n}{n+1}V_0 wR_{\text{ext}}(\pi-\Phi) \\
&+ m\frac{2}{\sqrt{3}}\frac{k\varepsilon_f^n}{n+1}(\pi-\Phi)V_0 D\frac{R_{\text{int}} + \frac{D}{2}\left[1-\cot\left(\frac{\Phi}{2}+\frac{\Psi}{2}\right)\tan\left(\frac{\Phi}{2}\right)\right]}{\sin\left(\frac{\Phi}{2}+\frac{\Psi}{2}\right)} + m\frac{k\varepsilon_f^n}{\sqrt{3}}V_0(2wL_{\text{exit}} + wL_{\text{ext}} + 2DL_{\text{exit}} + DL_{\text{ext}})
\end{aligned}
$$

$$
\begin{aligned}
&= m\frac{\sigma_y}{\sqrt{3}}V_0\left(2wL_{\text{entrance}} + wD\cot\left(\frac{\Phi}{2}+\frac{\Psi}{2}\right) + 2DL_{\text{entrance}} + D^2\cot\left(\frac{\Phi}{2}+\frac{\Psi}{2}\right)\right) + m\frac{k\varepsilon_f^n}{\sqrt{3}}V_0\left(2wL_{\text{exit}} + wD\cot\left(\frac{\Phi}{2}+\frac{\Psi}{2}\right) + 2DL_{\text{exit}}\right. \\
&\left. + D^2\cot\left(\frac{\Phi}{2}+\frac{\Psi}{2}\right)\right) + m\frac{1}{\sqrt{3}}\frac{k\varepsilon_f^n}{n+1}V_0 w(R_{\text{int}} + R_{\text{ext}})(\pi-\Phi) + m\frac{2}{\sqrt{3}}\frac{k\varepsilon_f^n}{n+1}(\pi-\Phi)V_0\left(\frac{R_{\text{int}} + R_{\text{ext}}}{2}\right)\frac{D}{\sin\left(\frac{\Phi}{2}+\frac{\Psi}{2}\right)}
\end{aligned}
\tag{A1}
$$

References

[1] Segal, V. M., 1981, "Plastic Working of Metals by Simple Shear," Russ. Metall., **1**, pp. 99–105.

[2] Gil Sevillano, J., van Houtte, P., and Aernoudt, E., 1980, "Large Strain Work Hardening and Textures," Prog. Mater. Sci., **25**, pp. 69–134.

[3] Luri, R., and Luis, C. J., 2006, "Study of ECAE Process by Using FEM," Mater. Sci. Forum, **526**, pp. 193–198.

[4] Iwahashi, Y., Wang, J., Horita, Z., Nemoto, M., and Langdon, T., 1996, "Principle of Equal-Channel Angular Pressing for the Processing of Ultra-Fine Grained Materials," Scr. Mater., **35**, pp. 143–146.

[5] Luis, C. J., 2004, "On the Correct Selection of the Channel Die in Equal Channel Angular Extrusion Processes," Scr. Mater., **50**, pp. 387–393.

[6] Luri, R., Luis, C. J., León, J., and Sebastián, M. A., 2006, "A New Configuration for Equal Channel Angular Extrusion Dies," ASME J. Manuf. Sci. Eng., **128**, pp. 860–865.

[7] Luis Pérez, C. J., and Luri, R., "Study of the ECAE Process by the Upper Bound Method Considering the Correct Die Design," Mech. Mater., in press.

[8] Nyung, D., 2000, "An Upper-Bound Solution of Channel Angular Deformation," Scr. Mater., **43**, pp. 115–118.

[9] Luis, C. J., 2004, "Upper Bound Analysis and FEM Simulation of Equal Fillet Radii Angular Pressing," Modell. Simul. Mater. Sci. Eng., **12**, pp. 205–214.

[10] Altan, B. S., Purcek, G., and Miskioglu, I., 2005, "An Upper-Bound Analysis for Equal-Channel Angular Extrusion," J. Mater. Process. Technol., **168**, pp. 137–146.
[11] Kobayashi, S., Oh, T., and Atlan, B. S., 1989, *Metal Forming and the Finite-Element Method*, Oxford University Press, New York.
[12] Luri, R., Leon, J., Luis, C. J., and Puertas, I., 2004, "Mechanical Behaviour of an Al-Mg Alloy Processed by ECAE," *The 21st International Manufacturing Conference IMC 21*, P. Phelan, ed., Vol. 1, pp. 167–174.